



0031-3203(94)00116-2

STATISTICAL GEOMETRICAL FEATURES FOR TEXTURE CLASSIFICATION

YAN QIU CHEN,* MARK S. NIXON and DAVID W. THOMAS

Department of Electronics and Computer Science, University of Southampton, U.K.

(Received 9 February 1994; in revised form 24 August 1994; received for publication 1 September 1994)

Abstract—This paper proposes a novel set of 16 features based on the statistics of geometrical attributes of connected regions in a sequence of binary images obtained from a texture image. Systematic comparison using *all* the Brodatz textures shows that the new set achieves a higher correct classification rate than the well-known Statistical Gray Level Dependence Matrix method, the recently proposed Statistical Feature Matrix, and Liu's features. The deterioration in performance with the increase in the number of textures in the set is less with the new SGF features than with the other methods, indicating that SGF is capable of handling a larger texture population. The new method's performance under additive noise is also shown to be the best of the four.

Texture analysis
Additive noise

Feature extraction

Statistical features

Geometrical features

1. INTRODUCTION

Texture plays an important role in image analysis and understanding. Its potential applications range from remote sensing, quality control, to medical diagnosis etc. As a front end in a typical classification system, texture feature extraction is of key significance to the overall system performance. Many papers have been published in this area, proposing a number of various approaches.

Structural approaches⁽¹⁻³⁾ are based on the theory of formal languages: a texture image is regarded as generated from a set of texture primitives using a set of placement rules. These approaches work well on "deterministic" textures but most natural textures, unfortunately, are not of this type.

From a statistical point of view, texture images are complicated pictorial patterns, on which, sets of statistics can be obtained to characterize these patterns. The most popularly used one is the Spatial Grey Level Dependence Matrix (SGLDM) method,^(4,5) which constructs matrices by counting the number of occurrences of pixel pairs of given gray levels at a given displacement. Statistics like contrast, energy, entropy and so forth are then applied to the matrices to obtain texture features. These statistics are largely heuristic, although Julesz's conjecture⁽⁶⁾ about the human eyes' inability to discriminate between textures differing only in third or higher order statistics is an indication of the appropriateness of the method. Other schemes include the Statistical Feature Matrix⁽⁷⁾ and the Texture Spectrum.^(8,9)

A two-dimensional power spectrum of a texture image often reveals the periodicity and directionality

of the texture. For example, a coarse texture tends to generate low frequency components in its spectrum while a fine texture will have high frequency components. Stripes in one direction cause the power spectrum to concentrate near the line through the origin and perpendicular to the direction. Fourier transform based methods^(10,11) usually perform well on textures showing strong periodicity, their performance significantly deteriorates, though, when the periodicity weakens.

Stochastic models such as two-dimensional ARMA, Markov random fields etc. can also be used for texture feature extraction via parameter estimation.⁽¹²⁻¹⁵⁾ These approaches consider textures as realizations of a random process. Structural and geometrical features appearing in textures are largely ignored. Other difficulties such as that in choosing an appropriate order for a model have also been reported.

This paper proposes a novel set of sixteen texture features based on the statistics of geometrical properties of connected regions in a sequence of binary images obtained from a texture image. The first step of the approach is to decompose a texture image into a stack of binary images. This decomposition has been proven to have the advantage of causing no information loss, and resulting in binary images that are easier to deal with geometrically. For each binary image, geometrical attributes such as the number of connected regions and their irregularity are statistically considered. Sixteen such statistical geometrical features are proposed in this paper.

2. THE STATISTICAL GEOMETRICAL FEATURES

An $n_x \times n_y$ digital image with n_l grey levels can be modelled by a 2D function $f(x, y)$, where $(x, y) \in$

* Author to whom all correspondence should be addressed.

$\{0, 1, \dots, n_x - 1\} \times \{0, 1, \dots, n_y - 1\}$, and $f(x, y) \in \{0, 1, \dots, n_l - 1\}$. $f(x, y)$ is termed the intensity of the pixel at (x, y) .

When an image $f(x, y)$ is thresholded with a threshold value α , $\alpha \in \{1, \dots, n_l - 1\}$, a corresponding binary image is obtained, that is

$$f_b(x, y; \alpha) = \begin{cases} 1 & \text{if } f(x, y) \geq \alpha \\ 0 & \text{otherwise} \end{cases}. \quad (1)$$

where $f_b(x, y; \alpha)$ denotes the binary image obtained with threshold α .

For a given original image, there are $n_l - 1$ potentially different binary images, i.e. $f_b(x, y; 1)$, $f_b(x, y; 2), \dots, f_b(x, y; n_l - 1)$. This set of binary images shall be termed a binary image stack. For images of a given size and of a given number of grey levels, the above defined mapping (of the space of images into the space of binary image stacks) is bijective (one-to-one and onto), which guarantees that no loss of information is entailed by this transform. This is true because

$$f(x, y) = \sum_{\alpha=1}^{n_l-1} f_b(x, y; \alpha)$$

$$\forall (x, y) \in \{0, 1, \dots, n_x - 1\} \times \{0, 1, \dots, n_y - 1\}. \quad (2)$$

For each binary image, all 1-valued pixels are grouped into a set of connected pixel groups termed connected regions. The same is done to all 0-valued pixels. (Appendix A presents formal definition and an algorithm.) Let the number of connected regions of 1-valued pixels in the binary image $f_b(x, y; \alpha)$ be denoted by $NOC_1(\alpha)$, and that of 0-valued pixels in the same binary image by $NOC_0(\alpha)$. Both $NOC_1(\alpha)$ and $NOC_0(\alpha)$ are functions of α , $\alpha \in \{1, \dots, n_l - 1\}$.

To each of the connected regions (of either 1-valued pixels or 0-valued pixels), a measure of irregularity (un-compactness) is applied, which is defined to be

$$\text{irregularity} = \frac{1 + \sqrt{\pi} \cdot \max_{i \in I} \sqrt{(x_i - \bar{x})^2 + (y_i - \bar{y})^2}}{\sqrt{|I|}} - 1, \quad (3)$$

where

$$\bar{x} = \frac{\sum_{i \in I} x_i}{|I|}, \quad \bar{y} = \frac{\sum_{i \in I} y_i}{|I|}, \quad (4)$$

I is the set of indices to all pixels in the connected region concerned, $|I|$ denotes the cardinality of the set I (the number of elements in I). (\bar{x}, \bar{y}) Can be thought of as the centre of mass of the connected region under the assumption that all the pixels in the region are of equal weight.

Alternatively, the usual measure of compactness (circularity) can be used, which is defined as

$$\text{compactness} = \frac{4\sqrt{|I|}}{\text{perimeter}}, \quad (5)$$

where

$$\begin{aligned} \text{perimeter} = & \sum_{i \in I} [f_b(x_i - 1, y_i) \oplus f_b(x_i, y_i) + f_b(x_i + 1, y_i) \\ & \oplus f_b(x_i, y_i) + f_b(x_i, y_i - 1) \oplus f_b(x_i, y_i) \\ & + f_b(x_i, y_i + 1) \oplus f_b(x_i, y_i)], \end{aligned} \quad (6)$$

\oplus denotes the logic XOR operator, that is

$$x \oplus y = \begin{cases} 1 & \text{if } x \neq y \\ 0 & x = y \end{cases}. \quad (7)$$

(Appendix B discusses the properties of the irregularity measure and the compactness measure in detail.)

As stated, a digital image corresponds to $n_l - 1$ binary images, each of which, in turn, comprises a few connected regions (of 1-valued pixels and of 0-valued pixels). Let the irregularity of the i th connected region of 1-valued pixels (0-valued pixels, respectively) of the binary image $f_b(x, y; \alpha)$ be denoted by $IRGL_1(i, \alpha)$ [$IRGL_0(i, \alpha)$, respectively]. The average (weighted by size) of irregularity of the regions of 1-valued pixels in the binary image $f_b(x, y; \alpha)$ is defined to be

$$\overline{IRGL}_1(\alpha) = \frac{\sum_{i \in I} [NOP_1(i, \alpha) \cdot IRGL_1(i, \alpha)]}{\sum_{i \in I} NOP_1(i, \alpha)}, \quad (8)$$

where $NOP_1(i, \alpha)$ is the number of pixels in the i th connected region of 1-valued pixels of the binary image $f_b(x, y; \alpha)$. $\overline{IRGL}_0(\alpha)$ is similarly defined.

By now, four functions of α , i.e., $NOC_1(\alpha)$, $NOC_0(\alpha)$, $IRGL_1(\alpha)$, $IRGL_0(\alpha)$, have been obtained, each of which, is further characterized using the following four statistics

$$\text{max value} = \max_{1 \leq \alpha \leq n_l - 1} g(\alpha), \quad (9)$$

$$\text{average value} = \frac{1}{n_l - 1} \sum_{\alpha=1}^{n_l-1} g(\alpha), \quad (10)$$

$$\text{sample mean} = \frac{1}{\sum_{\alpha=1}^{n_l-1} g(\alpha)} \sum_{\alpha=1}^{n_l-1} \alpha \cdot g(\alpha) \quad (11)$$

$$\text{sample S.D.} = \sqrt{\frac{1}{\sum_{\alpha=1}^{n_l-1} g(\alpha)} \sum_{\alpha=1}^{n_l-1} (\alpha - \text{sample mean})^2 \cdot g(\alpha)} \quad (12)$$

where $g(\alpha)$ is one of the four functions: $NOC_1(\alpha)$, $NOC_0(\alpha)$, $IRGL_1(\alpha)$, $IRGL_0(\alpha)$.

The same procedures apply if the alternative compactness measure is to be used. In all, there are 16 feature measures for a texture image, four obtained from $NOC_1(\alpha)$, four from $NOC_0(\alpha)$, four from $IRGL_1(\alpha)$, and another four from $IRGL_0(\alpha)$.

3. EXPERIMENTAL EVALUATION

3.1. The database

The set of all 112 texture pictures in the Brodatz's photographic atlas of textures was organized into three groups. The first group comprises four sets with each having 28 pictures, that is, the first set includes pictures D1 through D28, the second set includes pictures D29

through D56, and so on. The second group consists of two sets, the first set contains pictures D1 through D56, the second set contains pictures D57 through D112. The third group is made up of the whole set, namely, pictures D1 through D112. The database was arranged to ensure a systematic comparison of algorithms.

Each texture picture in the atlas was scanned by an HP flat bed scanner to produce a $256 \times 256 \times 8$ digital image, from which, sixteen $64 \times 64 \times 8$ sub-images were obtained using perfectly aligned 64×64 windows. Nine of them were then randomly chosen as samples. One sub-image for each texture is shown in Fig. C1 and C2 in appendix C.

3.2. Three other techniques for comparison

Three other methods along with the Statistical Geometrical Features (SGF) proposed in this paper were tested on the same aforementioned database under the same conditions for comparison.

(1) The Spatial Grey Level Dependence Matrix (SGLDM) approach (4) is popularly used for extracting texture features. Five commonly used features as suggested in (5): energy, entropy, correlation, local homogeneity and inertia were computed in our experiments.

(2) Liu's features (11) are one of the many methods based on the Fourier Transform. Eight optimal features (as proposed by the authors) $f_1, f_2, f_5, f_{17}, f_{20}, f_{21}, f_{25}, f_{26}$ were used.

(3) The recently proposed Statistical Feature Matrix (SFM) method (7) was claimed to have superior performance over SGLDM and Liu's features and therefore was considered in our experiments. The matrices M_{con} of size 4×4 and 8×8 were used.

There are 255 binary images obtainable from an 8-bit grey level digital image. To reduce computational costs, 63 binary images (evenly spaced thresholds, i.e. $\alpha = 4, 8, 12, \dots, 252$) were used in the experiments.

3.3. Feature normalization

All the features were standardized (normalized) by their sample means and S.D.'s which amounts to saying that every component was normalized using the following equation

$$f'_i = \frac{f_i - \mu}{\sigma}, \quad i = 1, 2, \dots, n, \quad (13)$$

where

$$\mu = \frac{1}{n} \sum_{i=1}^n f_i, \quad (14)$$

$$\sigma = \sqrt{\frac{1}{n} \sum_{i=1}^n (f_i - \mu)^2}, \quad (15)$$

n is the number of samples.

The k -nearest neighbour rule using the Euclidean distance and the "leave one out" estimate⁽¹⁶⁾ were then adopted for feature evaluation ($k = 3$). The k -nearest neighbour rule is popularly used in cases where the underlying probability distribution is unknown, and the "leave one out" estimate is unbiased and generally desirable when the number of available samples for each class is relatively small.

3.4. Classification results and discussions

On the first group of the four sets D1–D28, D29–D56, D57–D84 and D85–D112, it is seen from Table 1 that SGF's average correct classification rate is 92.1%, which is substantially higher than that of the other three techniques. A further look at the contingency tables (confusion matrices) as shown in Tables 2–5 gives more detailed information:

On the first set D1–D28, classification with SGF is accurate with the exception of misclassification on some rock/stone textures (D2, D5, D7, D23, D27 and D28) and tree bark textures (D12, D13). This is understandable because these rock/stone/tree bark images are non-stationary and its texture properties vary considerably with the location of the window; see Figure C1 in appendix. SFM's correct classification rate is a little higher than that of SGF on this set but it misclassifies nine textures into 12 wrong classes as against SGF's misclassifying eight textures into nine wrong classes. SGLDM's performance is poorer than the previous two. Liu's features can only correctly classify D1, D4, D8, D11 and D21.

On the second set D29–D56, SGF correctly classifies the textures with the exception of some misclassification between two similar pebbles D30 and D31 one on D50, and some misclassification among D43, D44 and D45 which is also understandable since D43, D44 and D45 contain patterns much larger than the window hence information obtainable within the window is inadequate. SFM's performance is considerably worse. It misclassifies several textures that are considerably

Table 1. Correct classification rates of various algorithms on the first group (four sets of 28 texture pictures)

	D1–D28	D29–D56	D57–D84	D85–D112	Average
SGF	90.8	92.6	93.5	91.5	92.1
SFM (4 × 4)	93.5	78.3	83.7	72.5	82.0
SFM (8 × 8)	93.1	80.8	81.7	70.1	81.4
SGLDM	88.4	83.9	76.6	79.2	82.0
Liu's features	62.3	57.4	38.8	42.4	50.2

SGF: SGF with the irregularity measure.

Table 2. Contingency tables on the first set D1–D28

classified as		true class																												
		D01	D02	D03	D04	D05	D06	D07	D08	D09	D10	D11	D12	D13	D14	D15	D16	D17	D18	D19	D20	D21	D22	D23	D24	D25	D26	D27	D28	
SGF		9	8	9	9	7	9	8	9	9	9	9	9	9	9	9	9	9	9	9	9	9	9	9	9	9	9	9	9	9
SFM		9	5	7	1	9	8	1	9	9	9	9	9	9	9	9	9	9	9	9	9	9	9	9	9	9	9	9	9	9
SGLDM		9	5	7	9	5	9	8	9	9	9	9	9	9	9	9	9	9	9	9	9	9	9	9	9	9	9	9	9	9
Liu's features		9	6	4	3	3	9	3	6	4	9	8	1	9	1	2	1	2	3	1	2	3	1	2	3	1	2	3	4	1

SGF: SGF with the irregularity measure. SFM: SFM M_{con} of size 4×4 .

different, e.g. D30/D46 and D33/D40/D42. SGLDM's discriminating ability is also considerably lower than that of SGF. Liu's features can only correctly classify D29, D37, D47 and D48.

On the third set D57–D84, SGF's discrimination ability is considerably better than the other three techniques in terms of correct classification rates and numbers of textures misclassified. Misclassification with SGF happens on textures that contain very large patterns or appear severely non-stationary. The same is true on the fourth data set D85–D112.

An alternative assessment of feature vectors is based on their within-class and inter-class distance distributions. We wish that the within-class distances of a feature vector are small and the inter-class distances

are large, thus giving a small overlapping area, ideally zero, since the smaller the area the less possibly patterns are to be misclassified although the ordering might not be strict.

Figures 1–4 show the distance distributions with the four techniques on the four data sets. It is seen from Fig. 1 that, on the first data set D1–D28, the overlapping area with SGF is the smallest, and that SFM gives the second smallest overlapping area (slightly larger than that with SGF), indicating that SGF and SFM should be the best two for this data set. Figures 2–4 show that the overlapping areas with SGF are considerably smaller than that with the other techniques on the data sets D29–D56, D57–D84 and D85–D112, indicating that SGF's performance should be

Table 3. Contingency tables on the second set D29–D56

classified as		true class														classified as		true class																																												
		D29	D30	D31	D32	D33	D34	D35	D36	D37	D38	D39	D40	D41	D42	D43	D44	D45	D46	D47	D48	D49	D50	D51	D52	D53	D54	D55	D56	D29	D30	D31	D32	D33	D34	D35	D36	D37	D38	D39	D40	D41	D42	D43	D44	D45	D46	D47	D48	D49	D50	D51	D52	D53	D54	D55	D56					
SGF		9	7	2	9	9	9	9	9	9	9	9	9	9	9	9	9	9	9	9	9	9	9	9	9	9	9	9	9	9	SFM		9	1	1	1	1	1	1	1	1	1	1	1	1	1	1	1	1	1	1	1	1	1	1	1	1	1	1	1	1	1
classified as	true class	D29	D30	D31	D32	D33	D34	D35	D36	D37	D38	D39	D40	D41	D42	D43	D44	D45	D46	D47	D48	D49	D50	D51	D52	D53	D54	D55	D56	D29	D30	D31	D32	D33	D34	D35	D36	D37	D38	D39	D40	D41	D42	D43	D44	D45	D46	D47	D48	D49	D50	D51	D52	D53	D54	D55	D56					
SGLDM	true class	D29	D30	D31	D32	D33	D34	D35	D36	D37	D38	D39	D40	D41	D42	D43	D44	D45	D46	D47	D48	D49	D50	D51	D52	D53	D54	D55	D56	D29	D30	D31	D32	D33	D34	D35	D36	D37	D38	D39	D40	D41	D42	D43	D44	D45	D46	D47	D48	D49	D50	D51	D52	D53	D54	D55	D56					
Liu's features	true class	D29	D30	D31	D32	D33	D34	D35	D36	D37	D38	D39	D40	D41	D42	D43	D44	D45	D46	D47	D48	D49	D50	D51	D52	D53	D54	D55	D56	D29	D30	D31	D32	D33	D34	D35	D36	D37	D38	D39	D40	D41	D42	D43	D44	D45	D46	D47	D48	D49	D50	D51	D52	D53	D54	D55	D56					

SGF: SGF with the irregularity measure. SFM: SFM M_{con} of size 4×4 .

substantially better than the other techniques on the data sets.

Comparison of techniques was also done on larger data sets, viz. on the two sets D1–D56 and D57–D112 of 56 textures as well as on the set of the whole database D1–D112. Results are presented in Table 6 and Table 7. It is expected that the performance of all techniques decreases as the size of the set increases. From Tables 1–3, one sees that the performance drop of SGF is the smallest (6.5% drop from average 92.1% on sets of size 28 to 85% for SGF, 9.2% drop for SFM 4×4 , 9.0% drop for SFM 8×8 , 17.4% for SGLDM, and 17.5% for Liu's features) indicating that SGF can handle a larger texture population than the other methods, which is indeed desirable since there are thousands of natural textures.

3.5. Classification under additive noise

Classification under additive noise was also considered. Zero mean, uncorrelated, uniformly distributed noise was added to the testing images. From the results as shown in Tables 8–10, one naturally sees that the performance of all the methods deteriorates as the signal to noise ratio (SNR) decreases. On the first group of four sets of 28 textures, SGF's performance under 30 dB SNR is substantially better than the others; under 20 dB and 10 dB SNRs, SFM 8×8 's performance is comparable to that of SGF's whilst the others are considerably worse, showing that under severe noise, SFM 8×8 may perform as well as SGF. The same is true for the second and third group, illustrating that SGF's performance under additive

Table 4. Contingency tables on the third set D57–D84

classified as		SGF								SFM							
		true class				SGF				true class				SFM			
D57	9	1	1	1	1	1	1	1	1	1	1	1	1	1	1	1	1
D58	8	1	1	1	1	1	1	1	1	1	1	1	1	1	1	1	1
D59	7	1	1	1	1	1	1	1	1	1	1	1	1	1	1	1	1
D60	6	1	1	1	1	1	1	1	1	1	1	1	1	1	1	1	1
D61	5	1	1	1	1	1	1	1	1	1	1	1	1	1	1	1	1
D62	4	1	1	1	1	1	1	1	1	1	1	1	1	1	1	1	1
D63	3	1	1	1	1	1	1	1	1	1	1	1	1	1	1	1	1
D64	2	1	1	1	1	1	1	1	1	1	1	1	1	1	1	1	1
D65	1	1	1	1	1	1	1	1	1	1	1	1	1	1	1	1	1
D66	9	1	1	1	1	1	1	1	1	1	1	1	1	1	1	1	1
D67	8	1	1	1	1	1	1	1	1	1	1	1	1	1	1	1	1
D68	9	1	1	1	1	1	1	1	1	1	1	1	1	1	1	1	1
D69	2	1	1	1	1	1	1	1	1	1	1	1	1	1	1	1	1
D70	1	1	1	1	1	1	1	1	1	1	1	1	1	1	1	1	1
D71	9	1	1	1	1	1	1	1	1	1	1	1	1	1	1	1	1
D72	7	1	1	1	1	1	1	1	1	1	1	1	1	1	1	1	1
D73	1	1	1	1	1	1	1	1	1	1	1	1	1	1	1	1	1
D74	1	1	1	1	1	1	1	1	1	1	1	1	1	1	1	1	1
D75	9	1	1	1	1	1	1	1	1	1	1	1	1	1	1	1	1
D76	9	1	1	1	1	1	1	1	1	1	1	1	1	1	1	1	1
D77	9	1	1	1	1	1	1	1	1	1	1	1	1	1	1	1	1
D78	9	1	1	1	1	1	1	1	1	1	1	1	1	1	1	1	1
D79	9	1	1	1	1	1	1	1	1	1	1	1	1	1	1	1	1
D80	9	1	1	1	1	1	1	1	1	1	1	1	1	1	1	1	1
D81	8	1	1	1	1	1	1	1	1	1	1	1	1	1	1	1	1
D82	9	1	1	1	1	1	1	1	1	1	1	1	1	1	1	1	1
D83	9	1	1	1	1	1	1	1	1	1	1	1	1	1	1	1	1
D84	9	1	1	1	1	1	1	1	1	1	1	1	1	1	1	1	1
D57	5	1	1	1	1	1	1	1	1	1	1	1	1	1	1	1	1
D58	5	1	1	1	1	1	1	1	1	1	1	1	1	1	1	1	1
D59	5	1	1	1	1	1	1	1	1	1	1	1	1	1	1	1	1
D60	4	1	1	1	1	1	1	1	1	1	1	1	1	1	1	1	1
D61	3	1	1	1	1	1	1	1	1	1	1	1	1	1	1	1	1
D62	2	1	1	1	1	1	1	1	1	1	1	1	1	1	1	1	1
D63	2	1	1	1	1	1	1	1	1	1	1	1	1	1	1	1	1
D64	3	1	1	1	1	1	1	1	1	1	1	1	1	1	1	1	1
D65	3	1	1	1	1	1	1	1	1	1	1	1	1	1	1	1	1
D66	2	1	1	1	1	1	1	1	1	1	1	1	1	1	1	1	1
D67	2	1	1	1	1	1	1	1	1	1	1	1	1	1	1	1	1
D68	2	1	1	1	1	1	1	1	1	1	1	1	1	1	1	1	1
D69	1	1	1	1	1	1	1	1	1	1	1	1	1	1	1	1	1
D70	1	1	1	1	1	1	1	1	1	1	1	1	1	1	1	1	1
D71	1	1	1	1	1	1	1	1	1	1	1	1	1	1	1	1	1
D72	1	1	1	1	1	1	1	1	1	1	1	1	1	1	1	1	1
D73	5	1	1	1	1	1	1	1	1	1	1	1	1	1	1	1	1
D74	1	1	1	1	1	1	1	1	1	1	1	1	1	1	1	1	1
D75	9	1	1	1	1	1	1	1	1	1	1	1	1	1	1	1	1
D76	6	1	1	1	1	1	1	1	1	1	1	1	1	1	1	1	1
D77	9	1	1	1	1	1	1	1	1	1	1	1	1	1	1	1	1
D78	6	1	1	1	1	1	1	1	1	1	1	1	1	1	1	1	1
D79	1	1	1	1	1	1	1	1	1	1	1	1	1	1	1	1	1
D80	1	1	1	1	1	1	1	1	1	1	1	1	1	1	1	1	1
D81	1	1	1	1	1	1	1	1	1	1	1	1	1	1	1	1	1
D82	8	1	1	1	1	1	1	1	1	1	1	1	1	1	1	1	1
D83	9	1	1	1	1	1	1	1	1	1	1	1	1	1	1	1	1
D84	6	1	1	1	1	1	1	1	1	1	1	1	1	1	1	1	1

SGF: SGF with the irregularity measure. SFM: SFM M_{con} of size 4×4 .

noise is good and SFM 8×8 is comparable to SGF under severe noise.

3.6. Visual interpolations

There is some correspondence between the SGF features and human perception of a texture. Eight features derived from $NOC_1(\alpha)$, $IRGL_1(\alpha)$ reflect the attributes of the bright blobs in an image while another eight features derived from $NOC_0(\alpha)$, $IRGL_0(\alpha)$ are related to the properties of the dark blobs in the image. (Pixels of higher values are brighter.) As $NOC_1(\alpha)$ and $NOC_0(\alpha)$ are based on the number of blobs they reveal the granularity of the texture whilst $NOC_1(\alpha)$ and $NOC_0(\alpha)$ describe the roundness of the blobs and they therefore help determine whether the blobs look more like disks and those in D15 look more like rods.

Table 11 lists the first SGF features from textures D15, D31 and D101. It is observed that the maximum value of $NOC_1(\alpha)$ sorts the textures into the ascending order D31, D101, D15, which basically agrees with human perception of the granularity (of the bright blobs). The maximum value of $IRGL_1(\alpha)$ gives the order D101, D31, D15, which also agrees with the fact that the bright blobs in D101 look more like disks and those in D15 look more like rods.

The second eight SGF features from textures D09, D49 and D102 are listed in Table 12. It is observed, similarly, that the ascending order D102, D49, D09, sorted by the maximum value of $NOC_1(\alpha)$ is largely consistent with human perception of the granularity (of the dark blobs). The order D102, D09, D49, sorted by the maximum value of $IRGL_1(\alpha)$ is also consistent

Table 5. Contingency tables on the fourth set D85-D112

SGF		SFM	
classified as	true class	classified as	true class
D85 9	9	D85 9	9
D86 9	9	D86 9	9
D87 9	9	D87 9	9
D88 7 1 2	7	D88 1 1 1	1
D89 8 2	8	D89 2 6	6
D90 1 1 3 2	1	D90 1 3 4	1
D91 1 1 3	1	D91 2 3 4	2
D92 9	9	D92 9	9
D93 9	9	D93 9	9
D94 8	8	D94 9	9
D95 9 1	9	D95 9	9
D96 8	8	D96 8	8
D97 9 1	9	D97 3	3
D98 2 9 1	2	D98 2	4
D99 2 9	2	D99 3	4
Da0 7	7	Da0 7	7
Da1 9	9	Da1 7 1	7 1
Da2 9	9	Da2 2 8	2 8
Da3 9	9	Da3 8 1	8 1
Da4 9	9	Da4 1 8	1 8
Da5 1	1	Da5 7 2	7 2
Da6 8	8	Da6 2 7	2 7
Da7 9	9	Da7 4	4
Da8 9	9	Da8 2 4	2 4
Da9 9	9	Da9 4 2	4 2
Db0 9	9	Db0 5 7	5 7
Db1 9	9	Db1 3 1	3 1
Db2 9	9	Db2 2 8	2 8
D85 7	7	D85 7	7
D86 9	9	D86 9	9
D87 9	9	D87 9	9
D88 7 1 4	7	D88 4 1	1
D89 1 6 1	1	D89 1 3	1
D90 1 6 1	1	D90 6 3	1
D91 1 4	1	D91 2 1 1 3	1
D92 1 9	1	D92 1	1
D93 1 5	1	D93 3	6
D94 7	7	D94 6 2	1
D95 9	9	D95 1 7	1
D96 9	9	D96 1 4	3
D97 2 2	2	D97 1	1
D98 7 2	7	D98 3 1	1
D99 3 2 5	3	D99 1 1	1
Da0 2 5	2	Da0 1 5	1
Da1 8	8	Da1 3	1
Da2 1 9	1	Da2 2 4	1
Da3 9	9	Da3 7 4	7 4
Da4 9	9	Da4 1	1
Da5 2 5	2	Da5 1	1
Da6 2 2	2	Da6 1 2 2	1
Da7 8 2	8	Da7 1	1
Da8 1 6	1	Da8 2 2	2
Da9 9	9	Da9 3 1	3 1
Db0 9	9	Db0 3 2	3 2
Db1 9	9	Db1 1 1	1 1
Db2 8	8	Db2 1	1
D85 7	7	D85 7	7
D86 9	9	D86 9	9
D87 9	9	D87 9	9
D88 7 1 2	7	D88 1 1	1
D89 8 2	8	D89 1 5	1
D90 1 3 2	1	D90 3	1
D91 1 1 3	1	D91 2 4	1
D92 9	9	D92 1	1
D93 9	9	D93 1	1
D94 9	9	D94 3 1	3 1
D95 9	9	D95 6 3	6 3
D96 9	9	D96 3 2	3 2
D97 2 2	2	D97 1	1
D98 8 2	8	D98 1	1
D99 1 6	1	D99 1	1
Da0 9	9	Da0 1	1
Da1 9	9	Da1 1	1
Da2 9	9	Da2 1	1
Da3 9	9	Da3 2 3	2 3
Da4 9	9	Da4 1	1
Da5 2 5	2	Da5 1	1
Da6 1 2 2	1	Da6 2 2	2
Da7 1	1	Da7 1 1	1
Da8 2 2	2	Da8 3 1	3 1
Da9 3 1	3	Da9 3 2	3 2
Db0 3 2	3	Db0 1 1	1 1
Db1 4 2	4	Db1 1	1
Db2 3 3	3	Db2 4 2	4 2
D85 9	9	D85 9	9
D86 9	9	D86 9	9
D87 9	9	D87 9	9
D88 1 1 1	1	D88 1 1	1
D89 2 6	2	D89 1	1
D90 1 3 4	1	D90 2	2
D91 2 3 4	2	D91 1	1
D92 9	9	D92 1	1
D93 9	9	D93 1	1
D94 9	9	D94 3 1	3 1
D95 9	9	D95 6 3	6 3
D96 9	9	D96 3 2	3 2
D97 1	1	D97 1	1
D98 8 2	8	D98 1	1
D99 1 6	1	D99 1	1
Da0 9	9	Da0 1	1
Da1 9	9	Da1 1	1
Da2 9	9	Da2 1	1
Da3 9	9	Da3 2 3	2 3
Da4 9	9	Da4 1	1
Da5 2 5	2	Da5 1	1
Da6 1 2 2	1	Da6 2 2	2
Da7 1	1	Da7 1 1	1
Da8 2 2	2	Da8 3 1	3 1
Da9 3 1	3	Da9 3 2	3 2
Db0 3 2	3	Db0 1 1	1 1
Db1 4 2	4	Db1 1	1
Db2 3 3	3	Db2 4 2	4 2
D85 9	9	D85 9	9
D86 9	9	D86 9	9
D87 9	9	D87 9	9
D88 1 1 1	1	D88 1 1	1
D89 2 6	2	D89 1	1
D90 1 3 4	1	D90 2	2
D91 2 3 4	2	D91 1	1
D92 9	9	D92 1	1
D93 9	9	D93 1	1
D94 9	9	D94 3 1	3 1
D95 9	9	D95 6 3	6 3
D96 9	9	D96 3 2	3 2
D97 1	1	D97 1	1
D98 8 2	8	D98 1	1
D99 1 6	1	D99 1	1
Da0 9	9	Da0 1	1
Da1 9	9	Da1 1	1
Da2 9	9	Da2 1	1
Da3 9	9	Da3 2 3	2 3
Da4 9	9	Da4 1	1
Da5 2 5	2	Da5 1	1
Da6 1 2 2	1	Da6 2 2	2
Da7 1	1	Da7 1 1	1
Da8 2 2	2	Da8 3 1	3 1
Da9 3 1	3	Da9 3 2	3 2
Db0 3 2	3	Db0 1 1	1 1
Db1 4 2	4	Db1 1	1
Db2 3 3	3	Db2 4 2	4 2

SGF: SGF with the irregularity measure. SFM: SFM M_{con} of size 4×4 .

Table 6. Correct classification rates of various algorithms on the second group (two set of 56 texture pictures)

	D1-D56	D56-D112	Average
SGF	90.2	87.3	88.8
SFM (4×4)	82.9	73.8	78.4
SFM (8×8)	83.7	71.4	77.6
SGLDM	79.9	67.7	73.8
Liu's features	50.8	31.9	41.4

SGF: SGF with the irregularity measure.

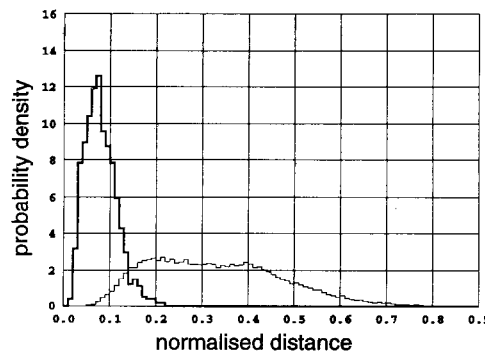
with the fact that the dark blobs in D102 are more like disks and those in D49 are more like-rod.

The other statistics, namely, the averages, means, and standard deviations of the functions are to help

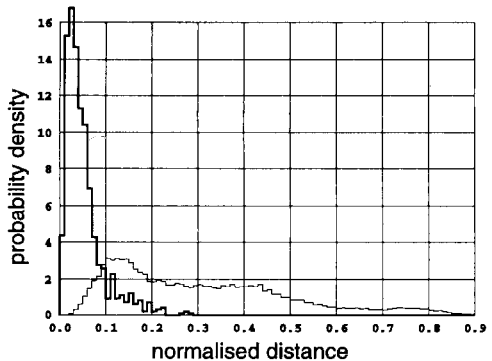
further characterize the functions. They have less obvious visual interpretations.

3.7. Computation time and storage requirements

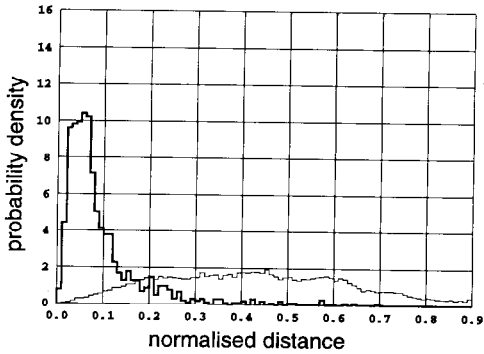
While the storage requirement of all the four techniques is in the order of tens of kilobytes, that is a small fraction of the amount accommodated by modern computers, computation time is a factor in choosing a technique. Table 13 lists the computation time required by the four methods to extract features from a 64×64 image. (The data is based upon the codes in C++ running on a 25 MHz 486.) The results suggest that SGF requires less computation time than Liu's features but more than SLDLM and SFM. In view of



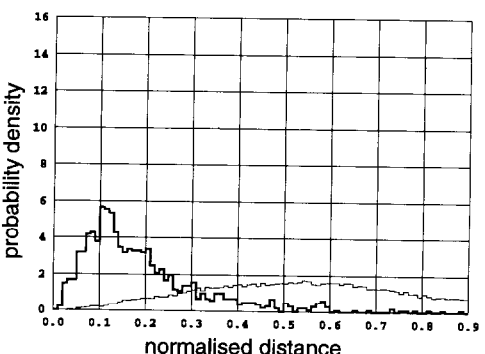
SGF



SFM

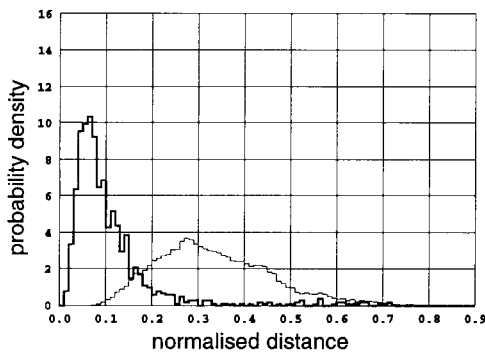


SGLDM

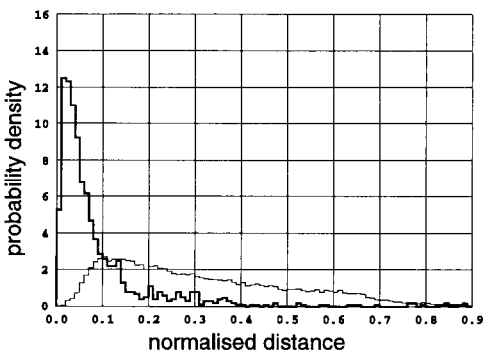


Liu's features

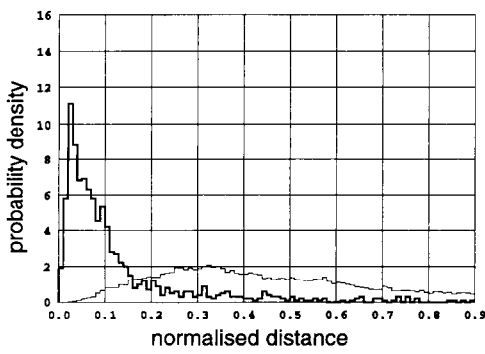
Fig. 1. Within-class (bold lines) and inter-class (fine lines) distance distributions on the first set D1–D28.
 SGF: SGF with the irregularity measure. SFM: SFM M_{con} of size 4×4 .



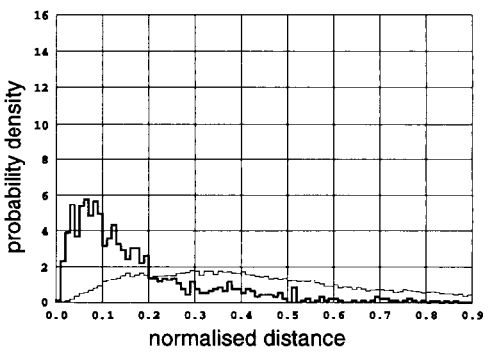
SGF



SFM

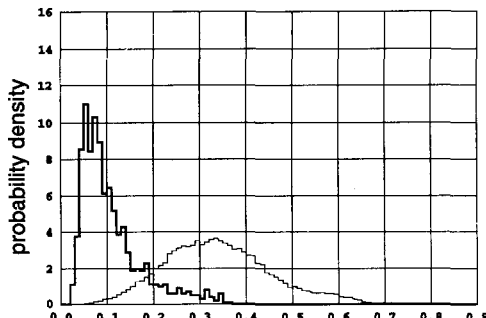


SGLDM

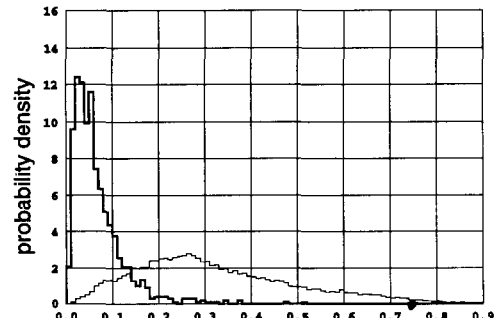


Liu's features

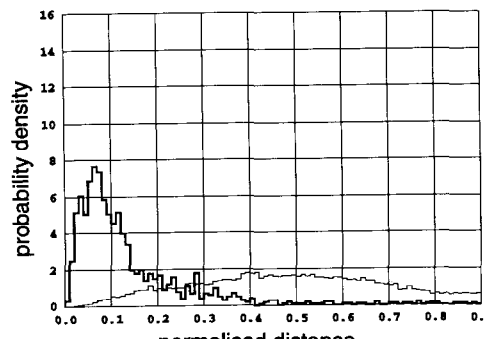
Fig. 2. Within-class (bold lines) and inter-class (fine lines) distance distributions on the second set D29–D56.
 SGF: SGF with the irregularity measure. SFM: SFM M_{con} of size 4×4 .



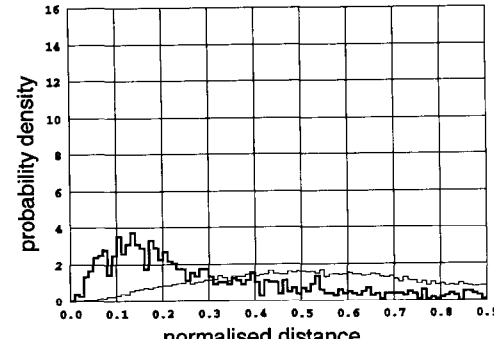
SGF



SFM

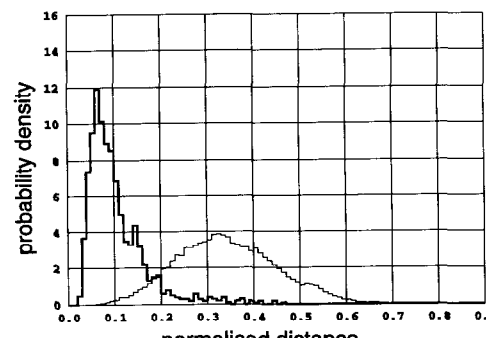


SGLDM

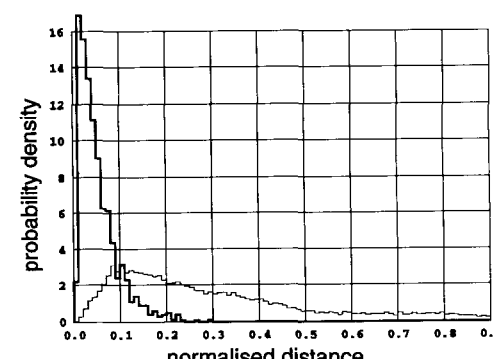


Liu's features

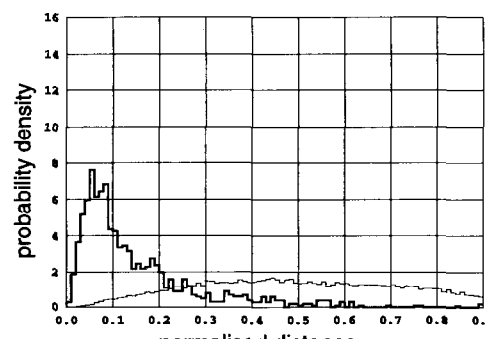
Fig. 3. Within-class (bold lines) and inter-class (fine lines) distance distributions on the third set D57–D84. SGF: SGF with the irregularity measure. SFM: SFM M_{con} of size 4×4 .



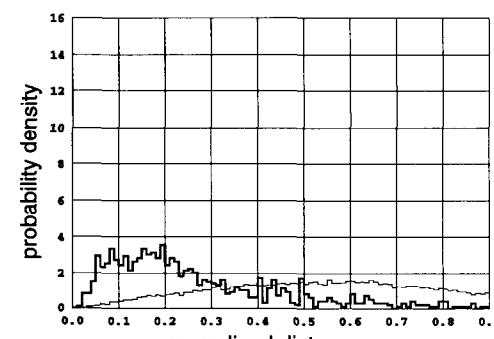
SGF



SFM



SGLDM



Liu's features

Fig. 4. Within-class (bold lines) and inter-class (fine lines) distance distributions on the fourth set D85–D112. SGF: SGF with the irregularity measure. SFM: SFM M_{con} of size 4×4 .

Table 7. Correct classification rates of various algorithms on the third group (one set of 112 texture pictures)

D1-D112	
SGF	85.6
SFM (4 × 4)	72.8
SFM (8 × 8)	72.4
SGLDM	64.6
Liu's features	32.7

SGF: SGF with the irregularity measure.

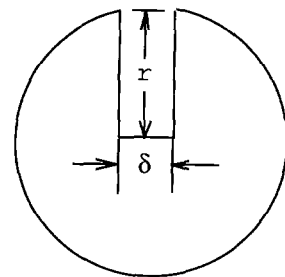


Fig. 5. A disk with a crack.

Table 8. Correct classification rates of various algorithms under additive noise on the first group (four sets of 28 texture pictures)

		D1-D28	D29-D56	D57-D84	D85-D112	Average
S/N = 30 (db)	SGF	91.1	91.1	92.0	90.8	91.3
	SFM (4 × 4)	93.1	78.3	82.4	72.1	81.5
	SFM (8 × 8)	92.6	80.8	82.4	71.0	81.7
	SGLDM	86.3	80.4	76.1	74.6	79.4
	Liu's features	61.8	54.7	37.9	39.5	48.5
S/N = 20 (db)	SGF	84.4	60.3	77.2	83.7	76.4
	SFM (4 × 4)	76.6	60.0	64.5	56.3	64.4
	SFM (8 × 8)	88.8	72.1	75.0	58.3	73.6
	SGLDM	57.1	45.5	55.1	39.1	49.2
	Liu's features	55.8	39.9	32.8	38.4	41.6
S/N = 10 (db)	SGF	24.6	8.3	22.1	35.9	22.7
	SFM (4 × 4)	20.5	16.1	14.3	10.9	15.5
	SFM (8 × 8)	24.1	23.0	17.4	17.0	20.4
	SGLDM	11.8	12.3	8.7	15.4	12.1
	Liu's features	11.8	10.3	10.9	8.4	10.3

SGF: SGF with the irregularity measure.

Table 9. Correct classification rates of various algorithms under additive noise on the second group (two sets of 56 texture pictures)

S/N = 30 (db)	SGF	89.1	86.6	87.9
	SFM (4 × 4)	82.3	73.5	77.9
	SFM (8 × 8)	83.5	72.0	77.8
	SGLDM	75.8	63.8	69.8
	Liu's features	49.0	31.3	40.2
S/N = 20 (db)	SGF	66.9	69.0	68.0
	SFM (4 × 4)	60.5	53.5	57.0
	SFM (8 × 8)	74.8	61.3	68.1
	SGLDM	42.2	37.5	39.9
	Liu's features	33.3	26.3	29.8
S/N = 10 (db)	SGF	14.4	20.8	17.6
	SFM (4 × 4)	16.4	5.7	11.1
	SFM (8 × 8)	20.5	11.0	15.8
	SGLDM	7.5	8.9	8.2
	Liu's features	5.7	3.9	4.8

SGF: SGF with the irregularity measure.

Table 10. Correct classification rates of various algorithms under additive noise on the third group (one set of 112 texture pictures)

		D1-D112
S/N = 30 (db)	SGF	84.0
	SFM (4 × 4)	71.4
	SFM (8 × 8)	72.3
	SGLDM	58.6
	Liu's features	31.3
S/N = 20 (db)	SGF	57.4
	SFM (4 × 4)	51.7
	SFM (8 × 8)	56.9
	SGLDM	28.7
	Liu's features	20.9
S/N = 10 (db)	SGF	13.6
	SFM (4 × 4)	9.1
	SFM (8 × 8)	13.6
	SGLDM	5.5
	Liu's features	3.1

SGF: SGF with the irregularity measure.

Table 13. Computation time of various algorithms

	Time (s)
SGF	1.5
SFM (4 × 4)	0.5
SFM (8 × 8)	1.0
SGLDM	0.3
Liu's features	2.5

SGF: SGF with the irregularity measure.

the Statistical Feature Matrix method and Liu's features—shows that the correct classification rate achieved by SGF proposed in the paper is substantially higher than that by the other three approaches, and that the reduction in performance with the increase in the number of textures in the set is slower with SGF than with the other three, indicating that SGF can handle a

Table 11. SGF features from D15, D31 and D101

	$NOC_1(\alpha)$				$IRGL_1(\alpha)$			
	av	max	mean	S.D.	av	max	mean	S.D.
D15	51.6	136.0	33.6	9.2	0.78	1.76	31.4	12.5
D31	10.2	25.0	29.1	11.7	0.56	1.03	27.2	13.0
D101	56.3	93.0	27.7	12.6	0.24	0.99	25.4	15.7

Av, Average; S.D., standard deviation

Table 12. SGF features from D09, D49 and D102

Texture	$NOC_1(\alpha)$				$IRGL_1(\alpha)$			
	av	max	mean	S.D.	av	max	mean	S.D.
D09	59.6	240.0	20.9	6.50	0.38	1.06	32.3	13.4
D49	13.9	112.0	12.0	9.51	1.56	5.18	17.6	11.2
D102	62.3	101.0	30.6	12.7	0.26	0.57	32.5	17.9

Av, Average; S.D., standard deviation

its superior performance (with respect to correct classification rates), SGF's computational costs may well be warranted.

4. CONCLUSIONS

A set of sixteen novel Statistical Geometrical Features (SGF) for texture analysis has been developed, which is based on the statistics of geometrical properties of connected regions in a sequence of binary images obtained from an original texture image. Systematic comparison using contingency tables of a k -nearest classifier and class distance distributions with the popularly-used Statistical Grey Level Dependence Matrix technique and two recently proposed methods—

larger texture population. SGF's performance under additive noise also compares favourably with the other three methods.

REFERENCES

1. S. Y. Lu and K. S. Fu, A syntactic approach to texture analysis, *Computer Graphics and Image Proc.* 7, 303–330 (1978).
2. L. Carlucci, A formal system for texture languages, *Pattern Recognition* 4, 53–72 (1972).
3. A. Accomazzi, A syntactic approach to the segmentation and classification of morphological features of galaxies, *Proc. of the SPIE* 1657, 534–545 (1992).
4. R. M. Haralick, K. Shanmugam and I. Dinstein, Textural features for image classification, *IEEE Trans. Syst. Man Cybernetics* 3, 610–621 (1973).

5. R. W. Connors and C. A. Harlow, A theoretical comparison of texture algorithms, *IEEE Trans. Pattern Analysis Mach. Intell.* **2**, 204–222 (1980).
6. B. Julesz, Visual pattern discrimination, *IRE Trans. Inf. Theory* **8**, 84–92 (1962).
7. C. M. Wu and Y. C. Chen, Statistical feature matrix for texture analysis, *CVGIP: Graphical Models Image Proc.* **54**, 407–419 (1992).
8. D. C. He and L. Wang, Texture unit, texture spectrum and texture analysis, *IEEE Trans. Geosci. Remote Sensing* **28**, 509–512 (1990).
9. D. C. He and L. Wang, Texture features based on texture spectrum, *Pattern Recognition* **24**, 391–399 (1991).
10. C. H. Chen, A study of texture classification using spectral features, *Proc. Sixth Int. Conf. Pattern Recognition* 1074–1077 (1982).
11. S. S. Liu and M. E. Jernigan, Texture analysis and discrimination in additive noise, *Computer Vision Graphics Image Proc.* **49**, 52–67 (1990).
12. M. Hassner and J. Sklansky, The use of markov random fields as models of texture, *Computer Graphics Image Proc.* **12**, 357–370 (1980).
13. H. Derin and W. Cole, Segmentation of textured images using gibbs random fields. *Computer Vision Graphics Image Proc.* **35**, 72–98 (1986).
14. F. S. Cohen, Z. Fan and M. A. Patel, Classification of rotated and scaled textured images using gaussian markov random field models. *IEEE Trans. Pattern Analysis Mach. Intell.* **13**, 192–202 (1991).
15. C. S. Won and H. Derin, Unsupervised segmentation of noisy and textured images using markov random fields. *CVGIP: Graphical Models Image Proc.* **54**, 308–328 (1992).
16. P. A. Devijver and J. Kittler, *Pattern Recognition: a Statistical Approach*. Prentice Hall International, Eagle Cliffs, New Jersey (1982).

APPENDIX A CONNECTIVITY

Definition 1. For a given coordinate pair (x, y) , the 4-neighbourhood is defined to be the set $N_4(x, y) = \{(x + 1, y), (x - 1, y), (x, y + 1), (x, y - 1)\}$.

Definition 2. A pixel p_1 at (x_1, y_1) is said to be a 4-neighbour of p_2 at (x_2, y_2) if and only if $(x_1, y_1) \in N_4(x_2, y_2)$.

Definition 3. Two pixels p and p' are 4-connected if and only if p is a 4-neighbour of p' and both the grey level l of p and the grey level l' satisfy some condition. e.g. they should be equal.

Definition 4. A 4-connecting path between p_1 and p_n is a sequence of pixels $(p_i)_{i=1}^n$ such that p_i and p_{i+1} for $1 \leq i \leq n - 1$ are 4-connected.

Definition 5. A 4-connected region is a set of pixels such that there is at least one 4-connecting path for each pair of pixels in this set.

A recursive algorithm for traversing a 4-connected region of gl-valued ($gl = 0$ or $gl = 1$) pixels around (x, y) is given as follows:

```
getConnectedRegion(int x, int y)
{
  if (imageArray[x][y] != gl) return;
  imageArray[x][y] = 1 - gl;
  addPixel(x, y);
  getConnectedRegion(x + 1, y);
  getConnectedRegion(x - 1, y);
  getConnectedRegion(x, y + 1);
  getConnectedRegion(x, y - 1);
  return;
}
```

where $imageArray$ is a two dimensional image array, $addPixel(int, int)$ is a function to store the pixels in a connected region for analysis.

To obtain all the connected regions from a binary image, one simply need to sequentially apply the above algorithm to every pixel of the image. It is easy to see that the computational complexity for obtaining all the connected regions in an image is $o(n)$ where n is the number of pixels in the image. In fact, no more than $6 \times n$ times accesses to $f(x, y)$ (an element of a two-dimensional array), arithmetic comparisons, and function calls are needed.

APPENDIX B. SHAPE MEASURES

Given a connected region A in the plane, the extent of its irregularity can be measured by the ratio of its maximum radius to the square root of its area, where the maximum radius is defined to be

$$r_{max} = \sup_{(x, y) \in A} \sqrt{(x - \bar{x})^2 + (y - \bar{y})^2}, \quad (B1)$$

$$\bar{x} = \frac{1}{A} \int x \, dx, \quad \bar{y} = \frac{1}{A} \int y \, dy. \quad (B2)$$

where \sup is supremum (the least upper bound).

Equation (3) (in main text) is for measuring the irregularity of a connected region in a digital image, where the factor $\sqrt{\pi}$ and two additive 1's are introduced to make the measure approximate to zero when the region is a disk (the most compact and hence least irregular region in the usual sense). This can be seen as

(1) If there is only one pixel in the region, equation (3) becomes

$$irregularity = \frac{1 + \sqrt{\pi} \cdot 0}{1} - 1 = 0 \quad (B3)$$

(2) As the space ε of the sampling grid [at spacing $(\varepsilon, \varepsilon)$] approaches 0 the irregularity of a disk becomes

$$irregularity = \lim_{\varepsilon \rightarrow 0} \left(\frac{1 + \sqrt{\pi} \cdot \max_{i \in I} \sqrt{(x_i - \bar{x})^2 + (y_i - \bar{y})^2}}{\sqrt{|I|}} - 1 \right) \\ = \lim_{\varepsilon \rightarrow 0} \left(\frac{1}{\sqrt{|I|}} + \sqrt{\pi} \cdot \frac{\max_{i \in I} \sqrt{(x_i - \bar{x})^2 + (y_i - \bar{y})^2}}{\sqrt{|I|}} - 1 \right) \\ = 0$$

$(|I|)$ approaches infinity as ε approaches 0.)

An alternative shape measure of a connected region in the plane is the ratio of the square root of its area to its perimeter, termed compactness or circularity. (The reciprocal of this measure constitutes a regularity measure that has the same properties to be discussed later.) Equation 5 (in main text) is given for measuring the compactness of a region in a digital image.

It is observed that the two measures, when applied to digital images, have their respective advantages and disadvantages as follows

(1) The irregularity measure is invariant to rotation while the compactness measure is not.

Proof. For a connected region A in the plane, a spatial sampling process using a grid of spacing $(\varepsilon, \varepsilon)$ gives rise to a corresponding region A_ε in a digital image. With moderate conditions upon A that are satisfied by most natural images, it is easy to see that as $\varepsilon \rightarrow 0$ the following independent of the rotation of A . (The area of a pixel is ε^2 , the height and width is ε .)

Table B1. Correct classification rates of SGF with the irregularity measure and that of SGF with the compactness measure on the first group (four sets of 28 texture pictures)

	D1–D28	D29–D56	D57–D84	D85–D112	Average
SGF (irregularity)	90.8	92.6	93.5	91.5	92.1
SGF (compactness)	91.3	89.7	92.9	92.4	91.6

(1a) The area of A_ε by counting the pixels in it approaches the area of A ;

(1b) the centre of mass of A_ε by using equation (4) approaches the centre of mass of A ;

(1c) the maximum radius of A_ε in equation (3) approaches the maximum radius of A .

Therefore the irregularity measure defined by equation (3) is independent of rotation.

The perimeter as measured using equation (7) for regions of some shape, however, is dependent on the angle of rotation. In fact, as $\varepsilon \rightarrow 0$, the measured perimeter approaches 4 for a unit square with sides parallel to the axes whilst the measured perimeter approaches $4\sqrt{2}$ for a unit square with diagonals parallel to the axes (rotated 45 degrees). As the measured area of A_ε approaches that of A as stated in (1a), the compactness measure gives a result $\sqrt{2}$ times larger for the original unit square than for the rotated square—a significant difference. \square

(2) The irregularity measure of a square is $(\sqrt{2\pi}/2) - 1 = 0.25$ while that of a disk is 0 as expected since a square is more irregular than a disk in the usual sense. However, the compactness measure of a square parallel to the axes is 1 while that of a disk is $(\sqrt{\pi}/2) = 0.89$, suggesting a square is more compact than a disk which is not usually acceptable.

(3) The compactness measure is more sensitive to a narrow crack in a region. The fact is demonstrated by considering a disk with a narrow crack as illustrated in Fig. 5. As δ tends to 0, the irregularity measure of the region converges to that of the same disk without the crack while the compactness measure converges to $(2/5)\sqrt{\pi} = 0.71$ —a value significantly different from the compactness measure of the same disk without the crack which is $(\sqrt{2}/2) = 0.89$. This suggests that

Table B2. Correct classification rates of SGF with the irregularity measure and that of SGF with the compactness measure on the second group (two sets of 56 texture pictures)

	D1–D56	D56–D112	Average
SGF (irregularity)	90.2	87.3	88.8
SGF (compactness)	90.1	87.9	89.0

Table B3. Correct classification rates of SGF with the irregularity measure and that of SGF with the compactness measure on the third group (one set of 112 texture pictures)

	D1–D112
SGF (irregularity)	85.6
SGF (compactness)	85.2

the irregularity measure tends to ignore narrow cracks whilst the compactness measure will register them—a potential advantage of the compactness measure.

Experimental results as shown in Tables B1–B3 are basically consistent with the theoretical analysis: the irregularity measure and the compactness measure give approximately the same performance as each has its own merits and shortcomings.

APPENDIX C. THE TEXTURE DATABASE

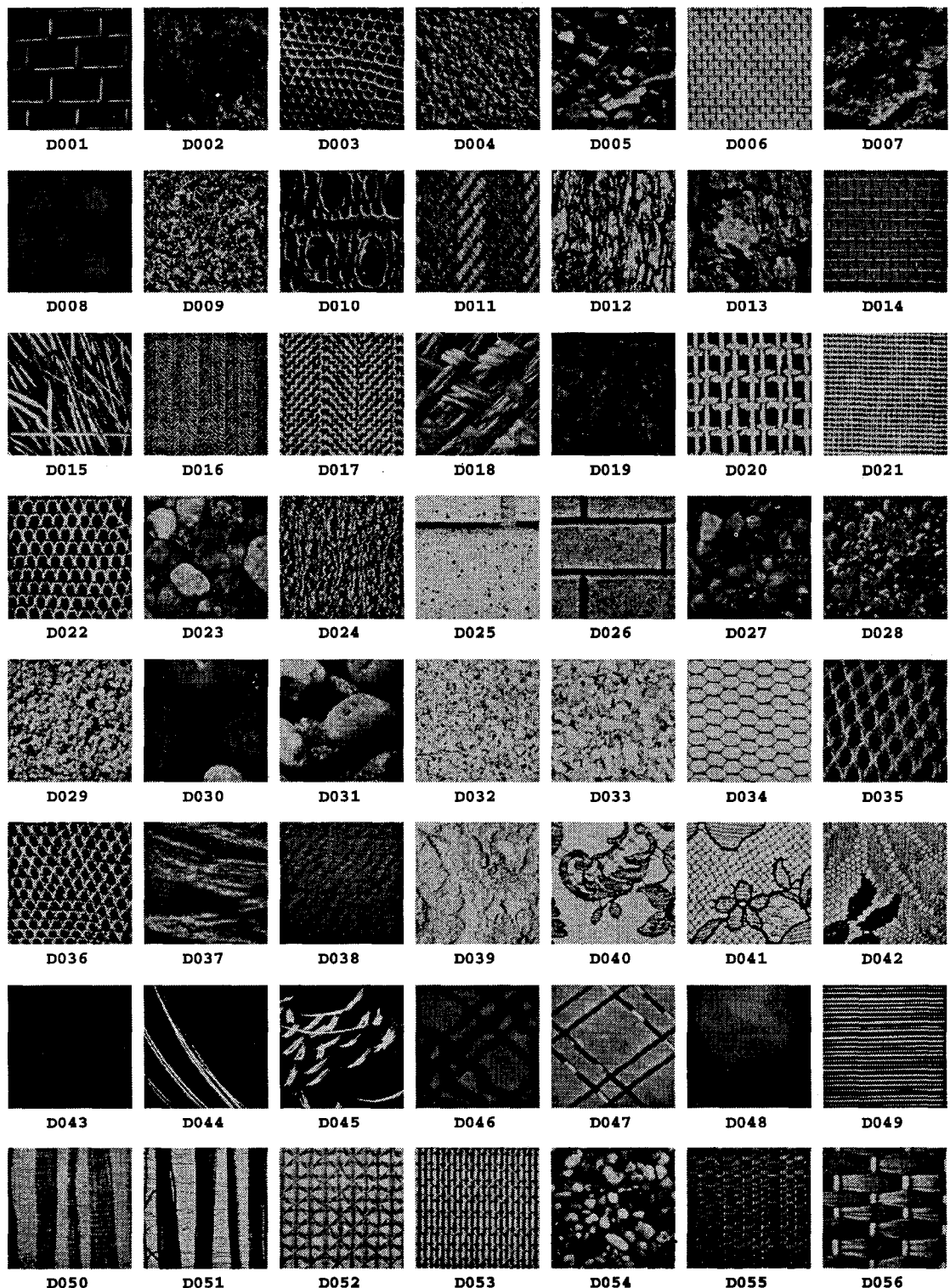


Fig. C1. Textures D1–D56.

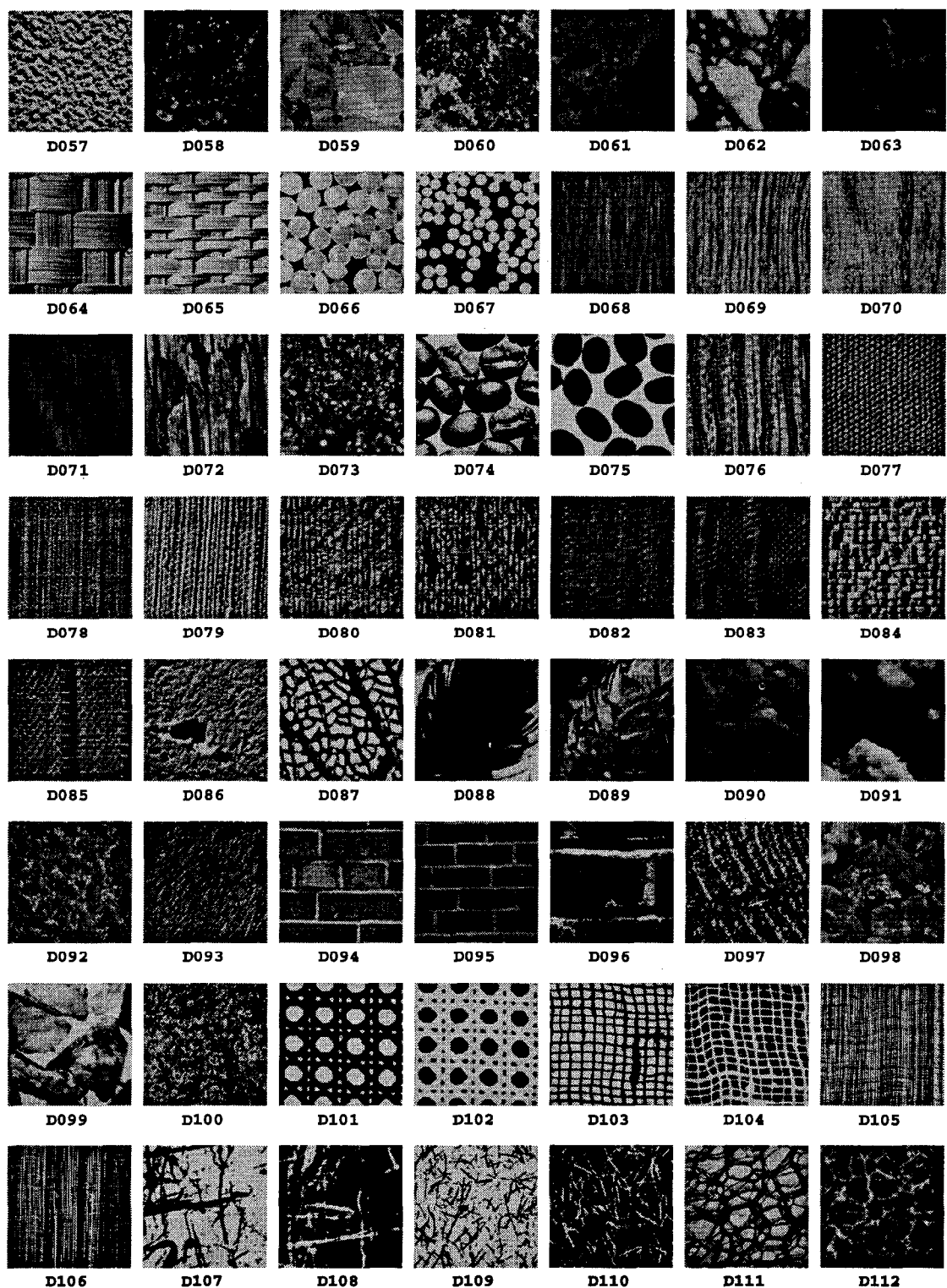


Fig. C2. Textures D57–D112.

About the Author—YAN QIU CHEN received his B.Eng and M.Eng in 1985 and 1988, respectively, from the Department of Electrical Engineering at Tongji University, Shanghai, P.R. China. He joined the Shanghai Maritime University in 1988, where he later became a research team leader in the Institute of Nautical Science and Technology. Mr Chen is currently a research student studying for a Ph.D. in the Vision Speech and Signal Processing (VSSP) research group in the Department of Electronics and Computer Science at Southampton University, U.K. His main research interests are in pattern recognition and neural networks.

About the Author—MARK NIXON is a lecturer in Electronics in Computer Science and is a member of the VSSP group. His research interests include computer vision and image processing with particular interests in feature extraction.

About the Author—DAVID THOMAS's research interests include signal processing both in 1 and 2D. His research has included vehicle identification, speech signal processing and image processing, including reconstruction and analysis.